Academic Journal of Science and Technology
ISSN: 2771-3032 | Vol. 8, No. 2, 2023

Design and Optimization Analysis of Downhole Robot Support Mechanism Based on Finite Element Method

Wei Wu, Xiaolin Ren, Yijun Liu, Pengpeng Zhang, Yu Li

School of Mechanical Engineering, Xi 'an Shiyou University, Xi 'an 710065, China

Abstract: To increase the traction force of the telescopic downhole robot, the support mechanism of the downhole robot was optimized, and a slider-spring transmission mechanism was introduced to solve the problem of jamming. A mathematical model of the support mechanism was established, covering the relationship between the contact normal pressure and the hydraulic cylinder load. The finite element simulation model of the friction block of the support mechanism was established based on Ansys software. Stress analysis of the casing under different contact normal pressures was carried out, and the frictional characteristics of the support mechanism friction block were obtained. The results show that the support mechanism composed of four linkages and friction locking blocks proposed in this paper can adapt well to casing of different diameters. The slider spring, as a transmission mechanism, has the elasticity and buffering effect, which makes the support mechanism have a certain flexibility, alleviating the vibration impact during obstacle crossing and reducing the impact on logging instruments. It enables the robot to passively adjust during obstacle crossing, effectively improving the traction capability of the downhole robot. Through finite element simulation, it was found that the depth of the plow groove produced by the friction block under normal pressure is basically proportional to the normal pressure. The greater the normal pressure, the deeper the plow groove, and the plow groove friction coefficient increases continuously with the increase of normal pressure, but the change in the plow groove friction coefficient gradually decreases as the pressure increases.

Keywords: Downhole robot; Finite element simulation; Optimization design; Support mechanism.

1. Introduction

The telescopic downhole robot is a robot used for downhole operations such as horizontal well drilling and logging. It has a large traction force and traction distance, which can solve the problem of insufficient traction force of traditional wheeled downhole robots in conveying continuous oil pipes and downhole operation instruments. However, the control system of the telescopic downhole robot is one of the key technologies for its underground operation. Currently, existing telescopic downhole robots face challenges such as complex support structure, jamming problems, and low control accuracy, which restrict their response speed and control precision. However, due to the confidentiality measures and high R&D costs of hydraulic telescopic downhole robot technology, its development in China is relatively lagging behind. Currently, research institutions and companies at home and abroad are increasing their research and application efforts on hydraulic telescopic downhole robots to promote further breakthroughs and applications of this technology.

This paper proposes a support mechanism composed of four linkages and friction locking blocks, which can adapt well to casing of different diameters. The slider spring, as a transmission mechanism, has the elasticity and buffering effect, which makes the support mechanism have a certain flexibility, alleviating the vibration impact during obstacle crossing and reducing the impact on logging instruments. It enables the robot to passively adjust during obstacle crossing. The frictional characteristics of the friction block support mechanism were obtained through finite element simulation.

2. Working Principle of Downhole Robot and Supporting Mechanism

2.1. Working principle of retractable underground robot

The telescopic downhole robot consists of two parts: the front working section and the rear working section. These two parts work independently and in coordination with each other. The working principle is as follows:

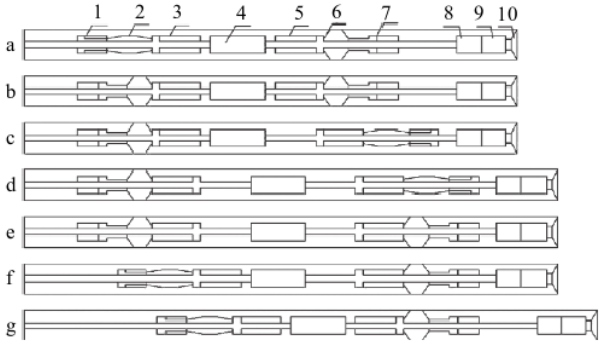

1. Left support cylinder; 2. Left support mechanism; 3. Left traction cylinder; 4. Control system; 5. Right traction cylinder; 6. Right support mechanism; 7. Right support cylinder; 8. Directional casing; 9. Power drilling tool; 10. Drill bit.

Figure 1. Working principle of telescopic downhole robot

The motion principle of the telescopic downhole robot is shown in Fig. 1. When crawling inside the wellbore or pipeline, the left and right working sections alternate to achieve telescopic crawling forward. One motion cycle can be divided into 7 motion steps. After completing one cycle of motion, the robot moves forward by the stroke of 2 telescopic

cylinders.

2.2. Working principle of the support mechanism

The friction locking block is designed based on the support structure of multi-link and four-link mechanisms with the casing wall. According to the driving principle of the motor-driven screw nut in existing downhole robots, a slider-spring transmission mechanism driven by a hydraulic cylinder is proposed. The support mechanism is shown in Figure 2, and it includes two steps:

(1) Support action: When the servo valve receives the control signal, it adjusts the spool displacement, causing the hydraulic cylinder piston rod to exert an output force F1, compressing the pressure spring and pushing the slider to slide in the piston sleeve. At the same time, the return spring is compressed, driving the right push rod to move to the left. This continues until the locking block completely contacts the casing wall, and the return spring is no longer compressed. As the piston rod continues to move, the pressure spring continues to compress, providing sufficient contact normal pressure for traction until the hydraulic cylinder piston stroke ends.

(2) Retraction action: When the servo valve receives the control signal, the solenoid valve switches, causing the hydraulic cylinder piston rod to move in the opposite direction, driving the slider to move the right push rod to the right. The return spring and pressure spring return to their initial state, and the hydraulic cylinder piston returns to its initial position.

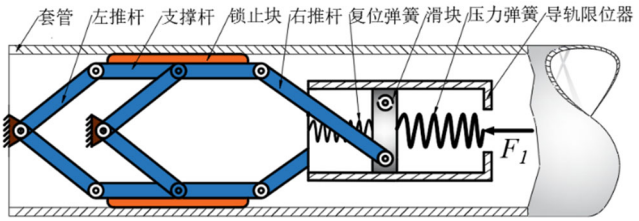

Figure 2. Working principle of hydraulic telescopic downhole robot support mechanism

The support structure proposed in this article, composed of a four-link mechanism and a friction locking block, is able to adapt well to different diameter casings. The slider spring, as a transmission mechanism, provides the support structure with elasticity and a cushioning effect, allowing it to have a certain degree of flexibility. This helps to alleviate vibration and impact during obstacle traversal, reducing the impact on logging instruments. It enables the robot to passively adjust during the obstacle traversal process.

3. Mechanical Modeling of Support Mechanism

3.1. Mechanical model of friction block support mechanism

According to the working principle of the support structure, the model is simplified to reduce its complexity, and a mechanics analysis is established as shown in Fig. 3. A coordinate system, xOy, is established with the fixed hinge of the left push rod as the origin, and the principle of virtual work is applied for the mechanics analysis.

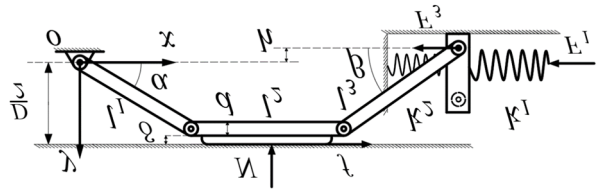

Figure 3. Mechanical analysis of friction block support mechanism

Where L_1 is the length of the left push rod, L_2 is the length of the support rod, L_3 is the length of the right push rod, L_4 is the length of the parallel rod, α is the angle between the left push rod and the horizontal direction, β is the angle between the right push rod and the horizontal direction,δ is the thickness of the locking block, D is the inner diameter of the casing, d is the diameter of the support rod, h is the offset between the right push rod and the horizontal direction at the hinge connecting the slider, k_1 is the spring stiffness of the pressure spring, k_2 is the spring stiffness of the reset spring, N is the contact normal pressure between the support structure and the casing wall, F_1 is the load force of the hydraulic cylinder, F_3 is the horizontal pushing force of the right push rod, and f is the traction force of the support structure.

The geometric relationships established according to Figure 3 are as follows: (followed by a description of the geometric relationships)

$$\begin{cases} S_x = L_1\cos\alpha + L_2 + L_3\cos\beta \\ S_y = L_1\sin\alpha + d/2 + \delta \\ L_1\sin\alpha + h = L_3\sin\beta \end{cases} \tag{1}$$

In the formula (1),

$$\begin{cases} sin\alpha = \frac{D-d}{2L_1} - \frac{h}{L_1} - \frac{\delta}{L_1} \\ sin\beta = \frac{D-d}{2L_3} - \frac{\delta}{L_3} \end{cases} \tag{2}$$

Total differentiation of the equation (1) is obtained:

$$\begin{cases} dS_x = -L_1\sin\alpha\, d\alpha - L_3\sin\beta\, d\beta \\ dS_y = L_1\cos\alpha\, d\alpha \\ L_1\cos\alpha\, d\alpha = L_3\cos\beta\, d\beta \end{cases} \tag{3}$$

According to the virtual work principle:

$$-NdS_y - F_3dS_x = 0 \tag{4}$$

Simultaneous (1), (3), (4) can be obtained:

$$N = F_3(tan\alpha + tan\beta) \tag{5}$$

In the formula,

$$\begin{cases} tan\alpha = \frac{\frac{D-d}{2}-h-\delta}{\sqrt{L_1^2-\left(\frac{D-d}{2}-h-\delta\right)^2}} \\ tan\beta = \frac{\frac{D}{2}-\delta}{\sqrt{L_3^2-\left(\frac{D}{2}-\delta\right)^2}} \end{cases} \tag{6}$$

The thrust of the right push rod of the support mechanism is:

$$F_3 = \frac{N}{\frac{\frac{D-d}{2}-h-\delta}{\sqrt{L_1^2-\left(\frac{D-d}{2}-h-\delta\right)^2}}+\frac{\frac{D}{2}-\delta}{\sqrt{L_3^2-\left(\frac{D}{2}-\delta\right)^2}}} \quad (7)$$

Therefore, the tractive force is:

$$f = \mu F_3(tan\alpha + tan\beta) \quad (8)$$

According to equation (8), it can be concluded that, under the condition of determining the parameters of the linkage, the main factor affecting the traction performance of the underground robot is the coefficient of friction, μ.

Neglecting the frictional force of the slider, the load force of the support cylinder is given by:

$$F_1 = k_1 \cdot \Delta x_1 = F_2 + F_3 = k_2 \cdot \Delta x_2 + F_3 \quad (9)$$

Using formula (8), we can obtain:

$$F_3 = \frac{f}{\mu(tan\alpha+tan\beta)} \quad (10)$$

Therefore, the hydraulic cylinder load is:

$$F_1 = \frac{f}{\mu(tan\alpha+tan\beta)} + k_2 \cdot \Delta x_2 \quad (11)$$

From the above equation, it can be seen that the locking of the support structure is related to the length of the support structure push rod, the thickness of the locking block, and the diameter of the pipeline. Increasing the spring force can increase the load force of the hydraulic cylinder. Under the same traction conditions and with a constant spring force, the larger the pipe diameter, the smaller the required load force of the hydraulic cylinder. If it is necessary to maintain a constant load force, the hydraulic cylinder needs to adjust the compression amount of the spring to increase the spring force.

4. Optimal Design of Support Mechanism

According to the API standard for oil casing, the material selected for the study is Q235 5"~7" casing. This means that it must satisfy the mechanical requirements of the minimum casing inner diameter for the structure, as well as the size requirements of the maximum casing inner diameter for the structure. Therefore, the support structure designed in this study has an adaptive adjustment function for the casing inner diameter.

For the 5"~7" casing inner diameter, the maximum traction force f_max for the telescopic downhole machine is 5000N. The friction angle φ between the locking block and the casing wall is 35°, and the friction coefficient is μ=0.7. Taking the example of a 110mm pipeline inner diameter, the maximum positive pressure of the support structure is approximately 7143N. Therefore, the positive pressure N generated between a single support foot and the pipeline should be greater than 3571.5N (assuming two support feet are symmetrically distributed).

4.1. Support Structure Optimization Design

To use a traction robot to perform horizontal well testing, it is necessary to design a structure with outer diameter dimensions and traction force that meet the requirements of horizontal well testing. In order to meet the special pipeline environment requirements for the robot in horizontal wells, the maximum traction force is achieved with the shortest axial length and the smallest outer diameter size. The structure of the traction force adjustment mechanism is complex, and in order to obtain the best combination of performance and structural parameters, the key parameters need to be optimized.

Optimization design variables for the multi-variable function with nonlinear constraints: [Not provided in the original text]

$$x = [x_1, x_2, x_3, x_4]^T = [L_1, L_2, L_3, h]^T \quad (12)$$

Objective function:

$$f(x) = min(f_3) = \frac{f}{\mu(tan\alpha+tan\beta)} \quad (13)$$

Constraints:

$$\begin{cases} \left(-L_1+L_2+L_3\right)^2-\left[h^2+\left(L_2+\sqrt{L_3^2-(\frac{D-d}{2}-\delta)^2}+\sqrt{L_1^2-(\frac{D-d}{2}-h-\delta)^2}\right)^2\right]<0 \\ L_1^2-\left[h^2+\left(L_2+\sqrt{L_3^2-(\frac{D-d}{2}-\delta)^2}+\sqrt{L_1^2-(\frac{D-d}{2}-h-\delta)^2}\right)^2\right]<0 \\ L_2^2-\left[h^2+\left(L_2+\sqrt{L_3^2-(\frac{D-d}{2}-\delta)^2}+\sqrt{L_1^2-(\frac{D-d}{2}-h-\delta)^2}\right)^2\right]<0 \\ L_3^2-\left[h^2+\left(L_2+\sqrt{L_3^2-(\frac{D-d}{2}-\delta)^2}+\sqrt{L_1^2-(\frac{D-d}{2}-h-\delta)^2}\right)^2\right]<0 \\ 10<h<L_1<\frac{D}{2}<L_3<L_2<L_4 \end{cases} \quad (14)$$

In this paper, the Angle α_0 between the support arm and the initial position of the horizontal axis is set to 15°. "Through MATLAB programming, fmincon() function toolbox is used to optimize the solution, and the results are as follows:

Table 1. Optimized parameters of support mechanism

Serial number	Main parameter	Value
1	L1/mm	54
2	L2/mm	85
3	L3/mm	80
4	h/mm	10
5	D/mm	110-150
6	d/mm	10
7	δ/mm	6
8	k_1/kN/m	10
9	k_2/kN/m	5

4.2. Mechanical analysis of the drive mechanism after optimization

After the parameter values of the drive mechanism are determined, k values of the optimized drive unit under different pipe diameters are calculated, and cftool toolbox in MATLAB is used to fit them. The fitting results are shown in Fig.4.

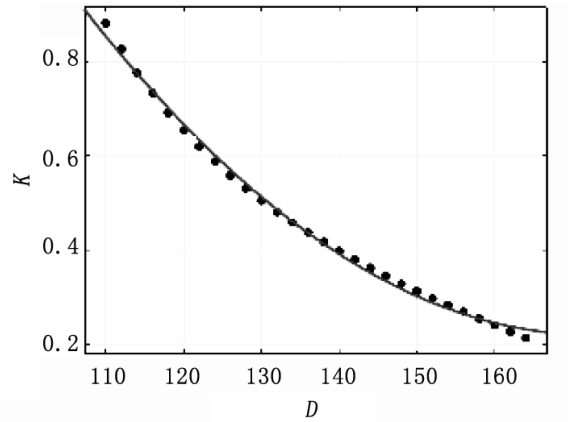

Figure 4. Polynomial curve fitting results

The fitting degree is 99.67%, and the function expression of F_1/N and pipe diameter is

$$= 0.0001623D^2 - 0.05599D + 5.048 \quad (15)$$

The relationship between the friction block spring force and the positive pressure can be expressed as

$$F_1 = (0.0001623D^2 - 0.05599D + 5.048) \cdot N \quad (16)$$

4.3. Optimization Feasibility Verification

In order to achieve a sufficiently large traction force, it is feasible to increase the normal pressure between the friction block and the pipe wall, thereby generating sufficient friction force between the support structure and the inner wall of the oil pipe. By combining multiple sets of driving short sections in a certain way, the load can be distributed to multiple support structures, achieving the goal of making the robot structure more compact. For downhole robots, during formal downhole operations, the required instrument string weight can be achieved by increasing the number of active short sections.

5. Finite Element Analysis of Support Mechanism Friction Blocks

5.1. Ploughing Effect

The traction force of underground robots mainly depends on the coefficient of friction between the friction blocks and the casing. There are many factors that affect the friction coefficient between the friction blocks and the casing. In order to increase the contact friction and improve the obstacle-surmounting ability, the friction blocks are often designed in a gear shape. Under a large positive pressure, the gear tips produce slight plastic deformation on the casing, resulting in very small grooves on the pipe arm. Therefore, traditional methods are not suitable for studying friction. The ploughing effect refers to the process in which rough peaks of hard metal are embedded into soft metal, causing the soft metal to flow and produce a groove. The research process in this paper uses a hexahedral tooth shape, which has better durability and stronger shear resistance compared to pointed teeth, resulting in less damage to the casing.

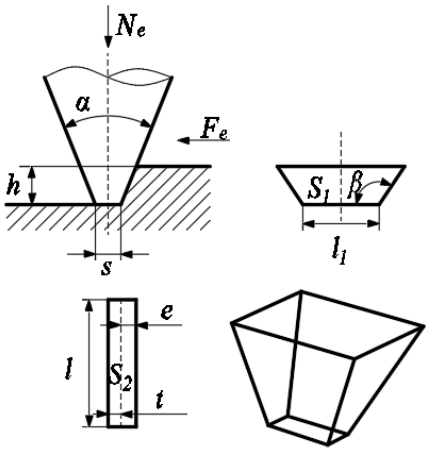

Figure 5. Schematic diagram of friction performance analysis of hexahedral drive wheel

The horizontal plane projection of the trapezoidal tooth contact surface of the hexahedron is a trapezoid, with the length of the lower side of the trapezoid being L_1, the indentation depth being h, the inclination angle of the friction block tooth being α, the top angle of the friction block tooth being β, and the friction force of the ploughing effect being F_e, then the horizontal plane projection area is: [The rest of the text seems to be a mathematical equation, which I cannot translate accurately without the specific symbols and context.]

$$S_1 = (h\,tan(\beta - 90°) + l_1)h \quad (17)$$

The contact area is projected as:

$$S_2 = (l_1 + 2h\,tan(\beta - 90°))\left(\frac{s}{2} + h\,tan\frac{\alpha}{2}\right) \quad (18)$$

Suppose the casing is an isotropic material and the positive pressure is:

$$N_e = S_2\tau_b \quad (19)$$

In the formula: τ_b—Embedded shear force, Pa, the value is approximately equal to the yield limit of the casing material.

The friction required for the furrow effect is:

$$F_e = S_1\sigma_s \quad (20)$$

In the formula: F_e—Furrow effect friction, N;

σ_s—Yield strength of casing material, Pa.

Therefore, the friction coefficient of the furrow effect is:

$$\mu = \frac{F_e}{N_e} \quad (21)$$

Coupling (17) ~ (21) can obtain friction factors:

$$\mu = \frac{[l_1 + h\,tan(\beta - 90°)]h}{[l_1 + 2h\,tan(\beta - 90°)]\left(\frac{s}{2} + h\,tan\frac{\alpha}{2}\right)} \quad (22)$$

The equation shows that under the ploughing effect, the friction coefficient between the friction block and the casing is related to the top angle and inclination angle of the friction block tooth, the length of the lower side, and the embedding depth.

5.2. Finite Element Analysis

(1) Simulation Model Establishment and Import

Based on the previous section and referring to the simulation conclusions of other scholars, this paper establishes a simulation analysis of a friction block with l_1=4mm, α=60°, β=120°, s=0.02mm. The friction block and pipeline models are created in Solidworks and saved in Parasolid (*.x-t) format, then imported into the Workbench finite element software. In Figure 6, (a) shows the overall model of the friction block, and (b) shows the finite element simulation model. The finite element simulation model simplifies the friction block to a single tooth, allowing for improved simulation accuracy by increasing mesh density while reducing computational simulation time to enhance efficiency.

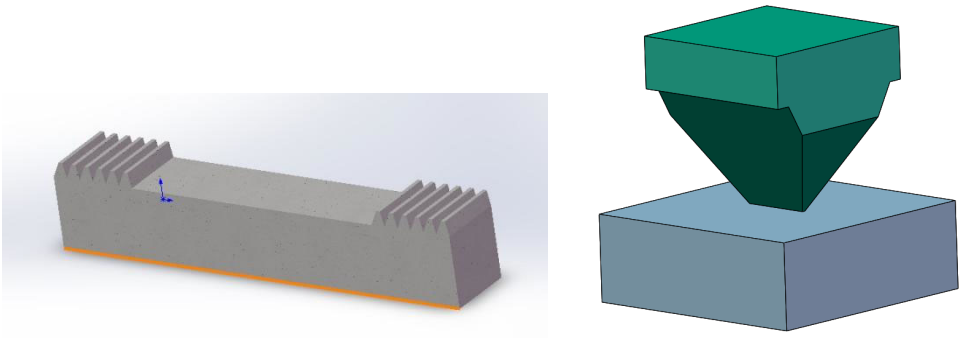

(a) Friction block model (b) Finite element simulation model

Figure 6. Friction block model and simulation modelDefine material propertiesDefine material properties

The material properties are set in the static analysis module. The friction block material is 40CrMoTi and the casing material is J55 (Q235). The corresponding material performance parameters [47] are shown in Tab.2:

Table 2. Mechanical properties parameters of driving wheel and casing materials

Name	Materials	Density /(kg/m^3)	Modulus of elasticity /GPa	Poisson's ratio	Yield strength /MPa
Friction block	40GrMoTi	7850	210	0.3	835
Cannula	J55 (Q235)	7800	200	0.28	235

(2) Mesh Division and Boundary Condition Settings

In Workbench, a hexahedral mesh is used with increased mesh density on the contact surface of the tooth, the four lateral surfaces, and the pipe surface to improve accuracy while reducing computation time. The mesh size is 0.5mm, with a refinement level of 3. The friction block tooth is set as the contact surface, the pipe surface as the target surface, and a fixed constraint is applied to the lower surface of the casing. The friction block is set to move in the vertical direction and is fixed in other directions. A vertical downward pressure is applied to the friction block at values of 250N, 500N, 750N, 1000N, 1250N, 1500N, 1750N, 2000N, 2250N, 2500N, 2750N, and 3000N, respectively, to calculate the deformation of the pipe under the corresponding pressures.

(3) Simulation Results and Friction Characteristics Analysis

According to the simulation results, the cloud image of pipeline deformation under corresponding positive pressure is shown in Figure 7.

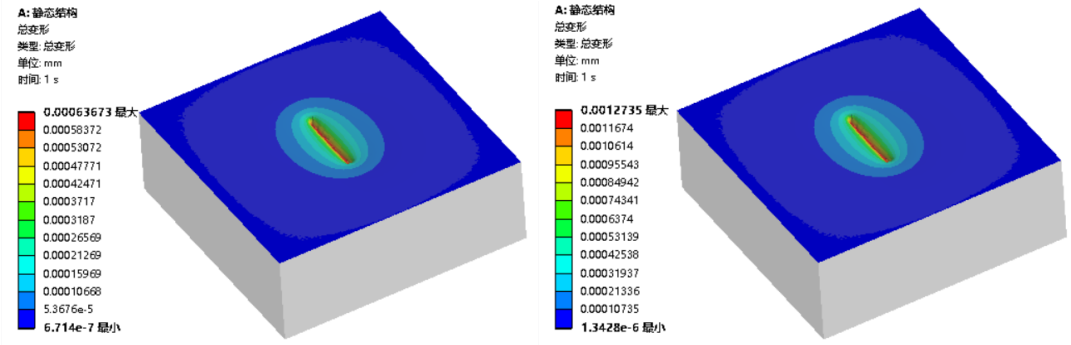

(a)250N (b)500N

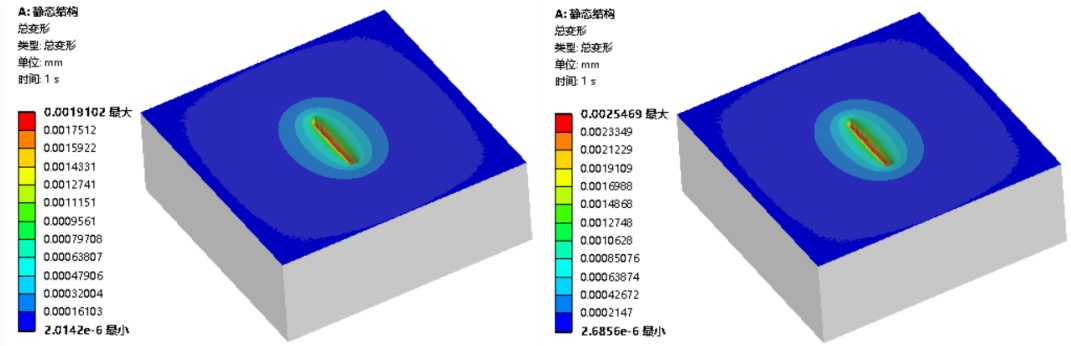

(c)750N

(d)1000N

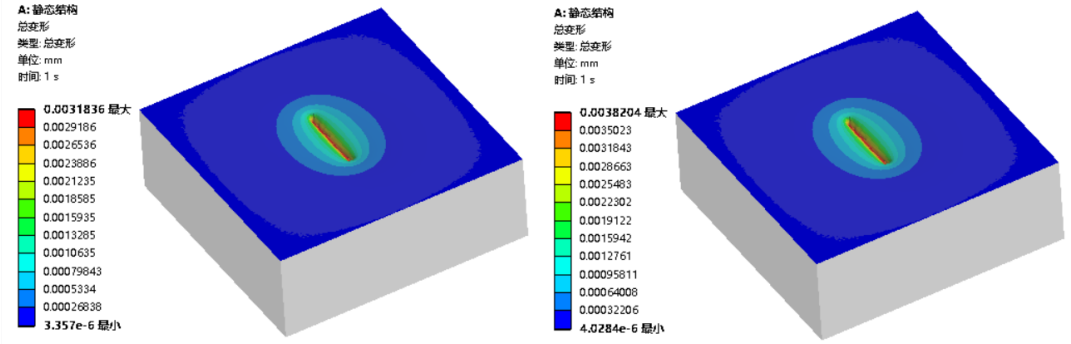

(e)1250N

(f)1500N

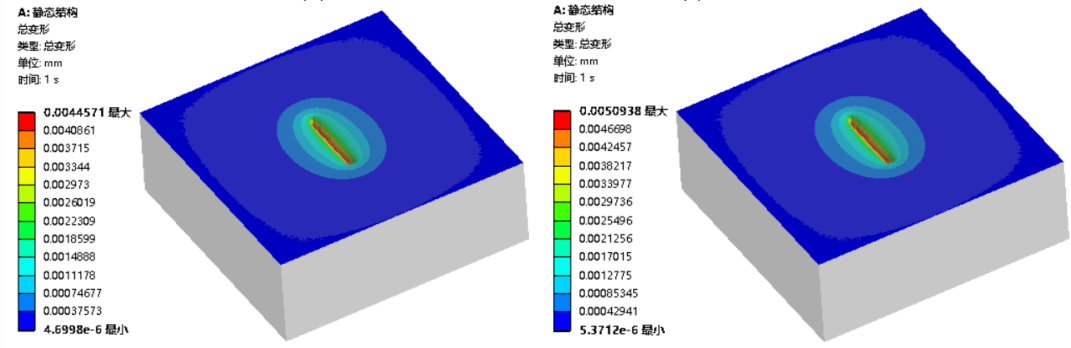

(g)1750N

(h)2000N

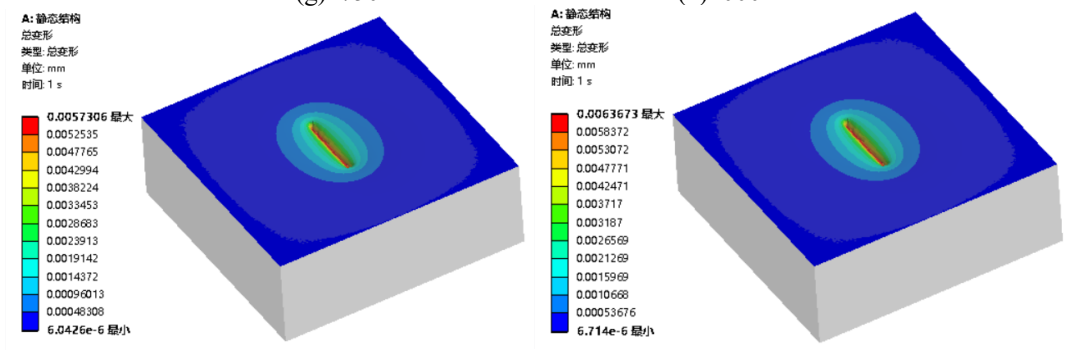

(i)2250N

(j)2500N

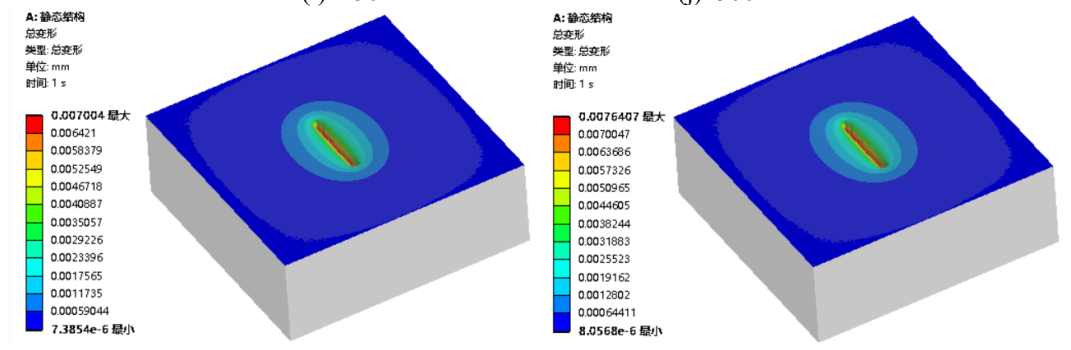

(k)2750N

(l)3000N

Figure 7. Cloud image of pipeline deformation under positive pressure

According to the pipe deformation cloud map and equation (22) in Figure 6, the furrow friction coefficient of the friction

block under corresponding positive pressure can be obtained, and the specific value is shown in Tab. 3.

Table 3. Pipeline deformation and corresponding furrow friction coefficient under positive pressure of friction block

Positive pressure /N	Furrow depth /mm	Friction coefficient of furrow	Positive pressure /N	Furrow depth /mm	Friction coefficient of furrow
250	0.00067373	0.2332	1750	0.0044571	0.8780
500	0.0012735	0.3936	2000	0.0050938	0.9335
750	0.0019102	0.5300	2250	0.0057306	0.9858
1000	0.0025469	0.6412	2500	0.0063673	1.0300
1250	0.0031836	0.7335	2750	0.0070040	1.0693
1500	0.0035023	0.7741	3000	0.0076407	1.1043

According to the results in Table 3, it can be concluded that when the friction block is subjected to pressure in the pipeline, the greater the pressure value, the deeper the furrow depth and the greater the friction coefficient of the furrow. The relationship between the positive pressure and the furrow depth-furrow friction coefficient is shown in Figure 8.

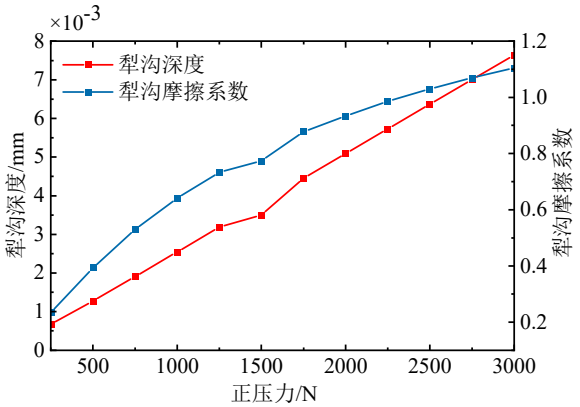

Figure 8. Furrow depth and furrow friction coefficient generated by friction block under positive pressure

Based on Figure 8, it can be concluded that the depth of the furrow produced by the friction block under positive pressure is proportional to the magnitude of the positive pressure. The greater the positive pressure, the deeper the furrow. The friction coefficient of the furrow increases continuously with the increase of the positive pressure. However, as the pressure increases, the magnitude of the change in the friction coefficient of the furrow gradually decreases.

6. Conclusion

A simplified mechanical model of the support mechanism for the telescopic downhole robot was established. Through optimized design, the best dimensions for the support mechanism within the 5" to 7" casing range were obtained, requiring minimal spring force and achieving maximum driving efficiency. The values for the linkagesL_1 and L_2were determined to maximize transmission efficiency based on the minimum ratio of spring force to positive pressure. By providing the functional relationship between spring force and positive pressure, the mechanical analysis and calculation of the driving structure were simplified. Finally, the relationship between the depth of the furrow produced by the friction block under positive pressure and the magnitude of the positive pressure was verified. It was found that the greater the positive pressure, the deeper the furrow, and the friction coefficient of the furrow increases continuously with the increase of the positive pressure, but the magnitude of the change in the friction coefficient gradually decreases as the pressure increases.

References

[1] LIU Qingyou, Dong Run, Geng Kai et al. Research progress and application prospect of downhole robot [J]. Petroleum Drilling Technology,2019,47 (03) : 50-55.

[2] Zhou Liangliang. Oil Technology,2016,2:160.

[3] There are good things in 'morning and night'. Application and development of horizontal well drilling technology in petroleum exploration and development [J]. Journal of Shandong University of Science and Technology (Natural Science Edition), 2000(02):117-119.

[4] Li Xiangtao, Qin Yuqiao, Chen Siping, et al. Transportation Technology of horizontal well logging Instrument and Its Application [J]. China Petroleum Machinery, 2014,8:98-102.

[5] Xie Huixiang. Dynamics Modeling and Control System Design of Telescopic Pipeline Robot [D]. National University of Defense Technology, 2009.

[6] Liu Qingyou. Current status and development trend of oil and gas pipeline robot technology [J]. Journal of Xihua University (Natural Science Edition),2016,35(01):1-6.

[7] Jiang Baoyan. Discussion on petroleum logging technology [J]. Chemical Design Communication,2017,43(10):213.

[8] Zeng Huajun. Research on Key Technologies of drive system of horizontal well tractor [D]. Harbin Institute of Technology, 2010.

[9] Liu Qingyou, Li Weiguo. Research and application of downhole crawler in Sondex horizontal Wells [J]. Oil Drilling and Production Technology, 2008(05):115-117.

[10] Cao Shuaiyuan, Chen Xiaoqiao, Luo Yihua. Discussion on transportation technology of production logging instruments in horizontal Wells [J]. Science and Technology Outlook, 2015, 25(28):153.